High resolution study of isovector negative parity states in the $^{16}O(^3He,t)^{16}F$ reaction at 140 MeV/nucleon

H. Fujita,[1,2,*] G. P. A. Berg,[3,†] Y. Fujita,[4] J. Rapaport,[5] T. Adachi,[4,‡] N. T. Botha,[6] H. Fujimura,[3,§] K. Fujita,[3] K. Hara,[3,∥] K. Hatanaka,[3] J. Kamiya,[3,¶] T. Kawabata,[7] K. Nakanishi,[3,**] R. Neveling,[2] N. Sakamoto,[3] Y. Sakemi,[3,††] Y. Shimbara,[4,‡‡] Y. Shimizu,[3,**] F. D. Smit,[2] M. Uchida,[8,§§] T. Wakasa,[3,∥∥] M. Yoshifuku,[4] M. Yosoi,[8,‡] and R. G. T. Zegers[9]

[1]*School of Physics, University of the Witwatersrand, Johannesburg 2050, South Africa*
[2]*iThemba LABS, Somerset West 7129, South Africa*
[3]*Research Center for Nuclear Physics (RCNP), Ibaraki, Osaka 567-0047, Japan*
[4]*Department of Physics, Osaka University, Toyonaka, Osaka 560-0043, Japan*
[5]*Department of Physics, Ohio University, Athens, Ohio 45701, USA*
[6]*Department of Physics, University of Cape Town, Rondebosch 7701, South Africa*
[7]*Center for Nuclear Study (CNS), University of Tokyo, Bunkyo, Tokyo 113-0033, Japan*
[8]*Department of Physics, Kyoto University, Sakyo, Kyoto 606-8224, Japan*
[9]*National Superconducting Cyclotron Laboratory (NSCL), Michigan State University, East Lansing, MI 48824, USA*

(Received 27 August 2008; published 20 February 2009)

The isovector transitions from the ground state (g.s.) of ^{16}O to the negative parity states in ^{16}F, i.e., the $J^\pi = 0^-$ g.s., the 0.193 MeV, 1^- state, the 0.424 MeV, 2^- state, the 0.721 MeV, 3^- state, and the 4^- "stretched" state at 6.372 MeV, were studied by using a high resolution $^{16}O(^3He,t)^{16}F$ reaction at 140 MeV/nucleon. With the help of high energy resolution, these states were, for the first time, clearly resolved in a charge exchange reaction at an intermediate energy, which favorably excites spin-flip states. Angular distributions of the reaction cross sections were measured in the laboratory frame from 0° to 14°. Parameters of phenomenological effective interactions were derived so as to reproduce these angular distributions in distorted wave Born approximation (DWBA) calculations. The angular distribution of the 0^- state could be reproduced well at $\theta_{c.m.} < 10°$. The empirical values, however, are larger by a factor of 2–2.5 in the larger angle region, where the contribution of the so-called "condensed pion field" is expected. The high resolution also enabled the decay widths of these states to be measured.

DOI: 10.1103/PhysRevC.79.024314 PACS number(s): 21.10.Pc, 25.55.Kr, 27.20.+n

I. INTRODUCTION

The long range terms of the nucleon-nucleon interaction are mediated by means of one-pionexchange [1]. It is predicted that the effects of pion exchange are mainly reflected in the momentum transfer dependence of the spin-longitudinal response which is inaccessible by electro-magnetic probes. It has been suggested that at a momentum transfer q larger than 1 fm^{-1} there should be an enhancement of the spin-longitudinal response, relative to the spin-transverse response [2]. Therefore, it is of considerable interest to measure the nuclear response for a $J^\pi = 0^-$ transition, since it carries the intrinsic spin-parity of the pion and it is a pure spin-longitudinal transition [3].

The 0^- excitations are expected as a component of the giant spin-dipole resonance. They can be seen in charge-exchange (CE) reactions as well as proton inelastic scattering (p, p') as a broad bump. However, it usually overlaps with the $J^\pi = 1^-$ and 2^- components and it is therefore difficult to study the 0^- component separately [4,5].

Excitations of discrete 0^- states are expected in the CE as well as the (p, p') reactions starting from the ground state (g.s.) of the spin-saturated target nucleus ^{16}O with $J^\pi = 0^+$ and $T_z = 0$ where T_z is the third component of the isospin T and defined by $(N - Z)/2$. The 0^- states with $T = 0$ and $T = 1$ can be excited in the $^{16}O(p, p')$ reaction, while the 0^- state in ^{16}F having $T = 1$ can be excited in CE reactions. On the other hand, $\Delta L = 0$ spin excitations like $M1$ and Gamow-Teller (GT) transitions that are usually strong at around 0°, are suppressed in these reactions on the spin-saturated target nucleus ^{16}O.

*Present address: Research Center for Nuclear Physics (RCNP), Ibaraki, Osaka 567-0047, Japan; hfujita@rcnp.osaka-u.ac.jp.
†Present address: Department of Physics, University of Notre Dame, IN 46556, USA.
‡Present address: Research Center for Nuclear Physics (RCNP), Ibaraki, Osaka 567-0047, Japan.
§Present address: Laboratory of Nuclear Science, Tohoku University, Taihaku-ku, Sendai, Miyagi 982-0826, Japan.
∥Present address: KEK, Oho, Tsukuba, Ibaraki 305-0801, Japan.
¶Present address: Japan Atomic Energy Research Institute, Tokai, Ibaraki 319-1195, Japan.
**Present address: Center for Nuclear Study (CNS), University of Tokyo, Bunkyo, Tokyo 113-0033, Japan.
††Present address: Cyclotron and Radioisotope Center (CYRIC), Tohoku University, Aoba-ku, Sendai, Miyagi 980-8578, Japan.
‡‡Present address: Graduate School of Science and Technology, Niigata University, 8050 Ikarashi 2-no-cho, Nishi-ku, Niigata 950-2181, Japan.
§§Department of Physics, Tokyo Institute of Technology, O-okayama, Meguro, Tokyo 152-8550, Japan.
∥∥Present address: Department of Physics, Kyushu University, Hakozaki, Fukuoka 812-8581, Japan.

Using the ^{16}O(p, p') reaction, excitations of the 0^- states at 10.96 MeV ($T = 0$) and 12.80 MeV ($T = 1$) were studied at 65 MeV [6], 200 MeV [7], and 400 MeV [8]. In Refs. [6,7], the authors report that the angular distribution did not agree with the theoretically predicted cross sections and analyzing powers at $q > 1$ fm^{-1}. Recently, the ^{16}O(p, p') reaction was measured at $E_p = 295$ MeV [9]. About 20 % enhancement of the cross sections for the 12.80 MeV, $T = 1$, 0^- state at $q > 1$ fm^{-1} was found relative to the values calculated in a distorted wave impulse approximation (DWIA). This enhancement was reproduced by a further DWIA calculation using random-phase-approximation response functions including the effect of the Δ isobar excitation that can cause pionic enhancement.

The 0^- g.s. of ^{16}F is the isobaric analog state of the $T = 1$, 12.80 MeV 0^- state in ^{16}O. The 0^- transition to this state can be studied in (p, n)-type charge-exchange reactions on a ^{16}O target nucleus. The other spin-dipole components, the 193 keV, $J^\pi = 1^-$ state and the 424 keV, $J^\pi = 2^-$ state can also be observed simultaneously. The 3^- state also exists at 721 keV close to these states. We refer to these states as quartet states. It should be noted that high energy resolution is required to study these states. In addition, a 4^- state can be observed at 6372 keV. As will be discussed, it is expected that these states have almost pure shell-model (SM) configurations. Therefore, a more consistent analysis of angular distributions can be performed.

Results of ^{16}O(p, n) measurements to study these low-lying spin-dipole states have been reported in Refs. [10,11]. However, in order to achieve the necessary energy resolution, the measurements were performed at low incident energies of 35 MeV [10] and at 79 MeV [11]. It is reported in Ref. [10] that the measured cross sections of the 0^- state in the large momentum transfer region of $1.4 \leqslant q \leqslant 2.0$ fm^{-1} were much larger than the values calculated by DWBA. The authors concluded that the disagreement might be due to the effect of the pion field in nuclei. However, at 79 MeV [11] the measured cross sections were smaller compared to the calculation. The different conclusions at different energies suggest that the reaction mechanism is responsible. At low incident energies, the reaction mechanism may not be predominantly one step which makes the results of the simple DWBA calculations questionable and interpretation of the results difficult. In addition, for the measurement at 79 MeV [11], the energy resolution was not sufficient to separate the low lying states clearly and a rather critical peak fitting analysis to be applied, which introduces additional uncertainties. Sterrenburg *et al.* have reported the results for the ^{16}O(^{3}He,t) reaction at 81 MeV [12]. However, at this low incident energy of 27 MeV/nucleon, it is expected that the reaction mechanism is complicated, which usually hinders the extraction of any decisive conclusion.

The high resolution capability of the Grand Raiden spectrometer [13] made it possible to overcome these difficulties. We performed a high energy-resolution ^{16}O(^{3}He,t)^{16}F experiment at 140 MeV/nucleon. At this incident energy we believe that the reaction proceeds mainly by a simple one-step mechanism, since good proportionality was found between the cross sections at 0° and the values of reduced Gamow-Teller transition strength, B(GT) [14]. We used a lateral and angular dispersion-matched beam to obtain the required energy resolution needed to resolve the low-lying quartet states and the 4^- state at higher excitation energy. It is expected that the measurements of angular distributions for various J states are helpful for a better understanding of effective projectile-target interaction because each term of the effective interaction contributes to the cross sections differently in transitions to different J states. The measured cross sections for these negative parity states can be compared with calculated DWBA cross sections using optimized effective interactions.

The high energy resolution also allowed to observe the peak widths caused by the particle decay. By assuming a Breit-Wigner function for the peak shapes, we studied these widths for the low-lying quartet states.

II. EXPERIMENT

The ^{16}O(^{3}He,t)^{16}F experiment was performed at RCNP by using a 140 MeV/nucleon ^{3}He beam from the Ring Cyclotron [15]. The WS beamline [16] designed to realize the full dispersion matching, was to transport a ^{3}He beam onto the target. In order to achieve the required energy resolution and the horizontal scattering angle resolution, we realized lateral and angular dispersion matching conditions described in Ref. [17]. These matching conditions were achieved by using the *faint beam method* [18] in the beam tuning procedure. A polyethylene terephthalate (PET) film, which includes carbon, oxygen, and hydrogen, was used as a ^{16}O target. Since the reaction Q-values of ^{16}O and ^{12}C are −15.4 MeV and −17.4 MeV, respectively, no contamination peaks from ^{12}C are expected below $E_x = 2$ MeV in ^{16}F (see Fig. 1). Natural carbon contains 1.1 % of ^{13}C. We verified that excited states in ^{13}N do not affect us by a measurement using a polyethylene target. Other possible contributions from oxygen isotopes, ^{17}O ($Q = -3.3$ MeV) and ^{18}O ($Q = -2.2$ MeV) should be very small because their natural abundances are 0.04% and 0.2%, respectively. We used a target with 3.3 mg/cm^2 areal density

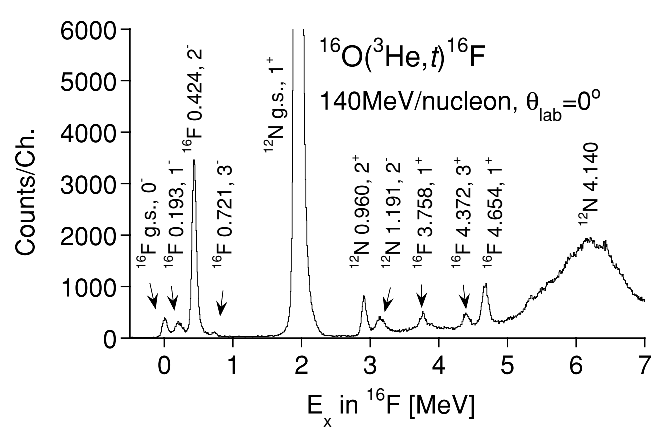

FIG. 1. Measured ^{16}O(^{3}He,t)^{16}F spectrum at 0° up to an excitation energy of about 7 MeV. Major states in ^{16}F are indicated by their excitation energies and J^π values. Several low-lying states in ^{12}N are also observed.

as a compromise between the conflicting requirements of high energy-resolution and a sufficiently high counting rate.

Outgoing tritons were momentum analyzed by the Grand Raiden magnetic spectrometer. The horizontal and vertical angular acceptances were ±20 mr and ±40 mr, respectively, defined by a rectangular aperture installed at the entrance of the spectrometer. For the 0° measurements the ^{3}He^{++} beam, having about half the magnetic rigidity ($B\rho$) of the tritons, was stopped in a Faraday cup placed inside the first dipole magnet of the spectrometer. For the measurements at 3°, the beam was stopped in a Faraday cup installed downstream of the first quadrupole magnet of the spectrometer. At angles larger than 6°, a standard Faraday cup in the scattering chamber was used.

The tritons were detected by two multiwire drift-chambers (MWDC) [19] placed along the focal plane with an angle of 45° relative to the central ray of the spectrometer. Each MWDC consisted of two anode wire planes, with one set of wires stretched vertically and another set of wires tilted at an angle of 48.2° with respect to the vertical direction. Two ΔE plastic scintillation detectors were installed downstream of the MWDCs. They were used for particle identification and the generation of fast timing signals to provide trigger signals. Data were taken from 0° to 14° in the laboratory frame, which corresponds to the momentum transfer range of 0 and 2 fm^{-1}. The spectrum up to 7 MeV excitation energy measured at 0° is shown in Fig. 1.

To achieve a good angular resolution in the vertical direction, the *over-focus mode* [20] of the Grand Raiden spectrometer was used. This together with *angular dispersion matching*, allowed the precise measurement of the scattering angles in both horizontal and vertical directions. The kinematic effects [18] in the horizontal as well as vertical directions can deteriorate the spacial resolution. Owing to the good angular resolutions, these effects were corrected. The higher-order aberrations of the spectrometer were minimized by using multipole magnets and were further corrected by the software. After these corrections were made in the offline analysis, a good energy resolution of 65 keV ($\Delta E/E = 1.5 \times 10^{-4}$) was achieved. The spectra of the low-lying quartet states at laboratory angles 0°, 6°, and 12° are shown in Fig. 2(a), 2(b), and 2(c), respectively. As can be seen, good separation of all peaks are realized.

To obtain the optical model (OM) potential parameters needed in the DWBA calculations, the ^{3}He elastic scattering cross sections for ^{16}O were measured in the laboratory angular range of 7° to 24°.

III. ANALYSIS AND DISCUSSION

The spectra were analyzed by peak deconvolution software to obtain peak intensities as well as widths [21]. The experimental peak shape of the strongly excited and well isolated ^{12}N g.s. without particle decay width observed in the same spectra from the PET film target was used as a reference. The intrinsic peak width Γ was derived by assuming a Breit-Wigner function. In order to obtain the absolute cross section accurately, the total detection efficiency of the MWDCs of about 80 % to 88 % was taken into account. The live time

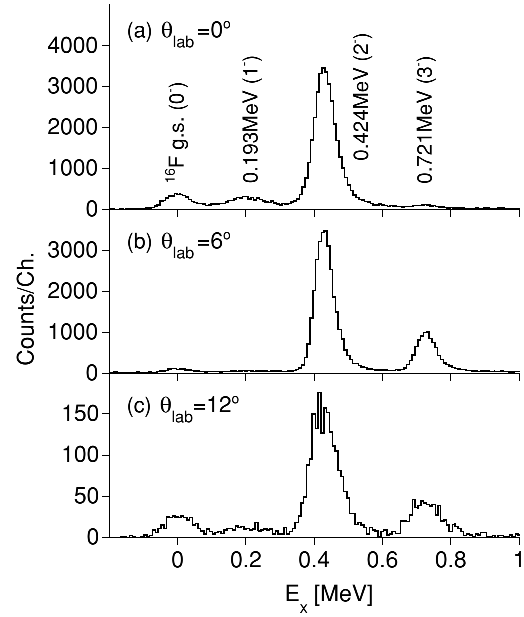

FIG. 2. Measured spectra of low-lying states in ^{16}F at 0°, 6°, and 12°. All states are clearly resolved.

ratios of the data acquisition system were about 96 % at 0° and 3°, and almost 100% at larger angles.

The measured angular distributions of the cross sections for the low-lying quartet states, i.e., the 0^- g.s., the 1^- state at 0.193 MeV, the 2^- state at 0.424 MeV, and the 3^- state at 0.721 MeV, as well as the stretched 4^- state at 6.372 MeV are shown in Fig. 3. These angular distributions were analyzed in the framework of DWBA calculations by using the simple and well used code DW81 [22]. The wave functions of the 0^-, 1^-, 2^-, and 3^- states for the DWBA calculation were obtained by using the code OXBASH [23]. The WBP interaction [24] was used and the SPSDPF model space was included. Transitions up to $1\hbar\omega$ were taken into account. Almost pure $(2s_{1/2},\ p_{1/2}^{-1})$ configurations were calculated for the transitions to the 0^- and 1^- states. Similarly almost pure $(d_{5/2},\ p_{1/2}^{-1})$ configurations were obtained for the transitions to the 2^- and 3^- states. It was assumed that the 4^- stretched state has a pure $(d_{5/2},\ p_{3/2}^{-1})$ configuration. The one-body transition densities for different transitions are summarized in Table I.

The OM potential parameters for ^{3}He were obtained by fitting the measured angular distribution of the differential

TABLE I. Deduced shell-model one-body transition densities for different configurations of the 0^-, 1^-, 2^-, 3^-, and 4^- states. For details of the calculations, see text.

	0^-	1^-	2^-	3^-	4^-
$(d_{5/2},p_{3/2}^{-1})$		0.119	−0.193	−0.133	1.0
$(d_{3/2},p_{3/2}^{-1})$	0.058	0.030	−0.029	−0.037	
$(2s_{1/2},p_{3/2}^{-1})$		0.001	−0.032		
$(d_{5/2},p_{1/2}^{-1})$			−0.980	0.990	
$(d_{3/2},p_{1/2}^{-1})$		0.082	0.007		
$(2s_{1/2},p_{1/2}^{-1})$	0.998	−0.989			

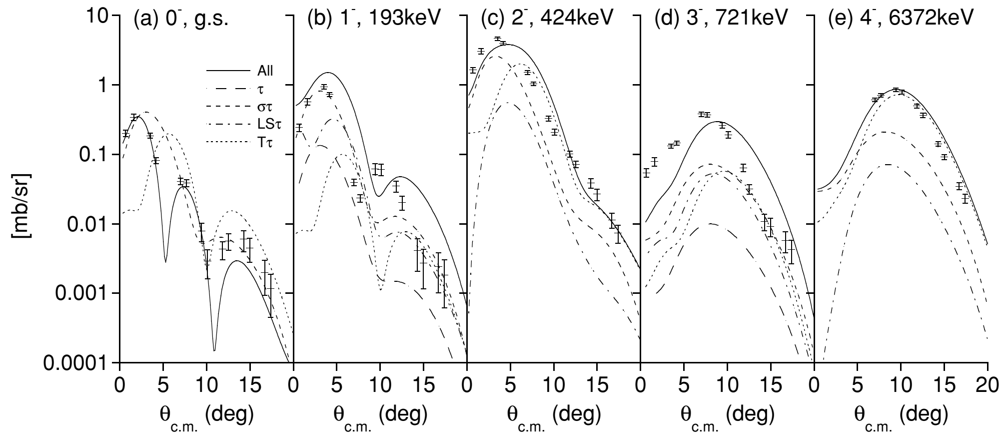

FIG. 3. The measured cross sections for transitions to the 0^-, 1^-, 2^-, 3^-, and 4^- states in ^{16}F. The results of the DWBA calculations are represented by solid lines. Longer and shorter dashed, dot-dashed and dotted lines show the contributions of the τ, $\sigma\tau$, $LS\tau$, and $T\tau$ terms of the effective interaction, respectively. For details of the calculations, see text.

cross sections of the ^{3}He elastic scattering data by using the code ECIS88 [25]. The resulting Woods-Saxon OM potential parameters are $V = 22.08$ MeV, $r_R = 1.54$ fm, $a_R = 0.74$ fm, $W = 42.66$ MeV, $r_I = 0.89$ fm, and $a_I = 0.96$ fm. In Refs. [26,27] at an energy very similar to the present experiment, i.e., at 150 MeV/nucleon, reported potential parameters were rather different from each other. It was found that the volume integrals of the present OM potentials were consistent with those given in Ref. [26]. For the outgoing tritons, following the argument given in Ref. [28], the well depths were multiplied by a factor of 0.85, while keeping the same geometrical parameters.

In the present analysis, we applied a simple form with a one-range Yukawa potential derived by Schaeffer [29] for the effective projectile-target interaction of the composite particle ^{3}He. The effective projectile-target interaction was described by isospin (τ), spin-isospin ($\sigma\tau$), LS-isospin ($LS\tau$), and tensor-isospin ($T\tau$) components. Contributions of the τ and $\sigma\tau$ components are expected to be larger than the others at small momentum transfer region (e.g., in Fermi and GT transitions) while the $T\tau$ and $LS\tau$ terms become stronger at relatively larger momentum transfer region [1]. The form of the interaction is given by

$$\begin{aligned} V_{\rm eff} = \{ & V_\tau Y(r/R_\tau) + V_{\sigma\tau}(\sigma_1 \cdot \sigma_2) Y(r/R_{\sigma\tau}) \\ & + V_\tau^{\rm LS}(\mathbf{L}\cdot\mathbf{S}) Y\left(r/R_\tau^{\rm LS}\right) \\ & + V_{T\tau} r^2 S_{12} Y(r/R_{T\tau})\}(\tau_1 \cdot \tau_2), \end{aligned} \tag{1}$$

where Y represents the Yukawa potential and S_{12} is the tensor operator defined by

$$S_{12} = \frac{3(\sigma_1 \cdot \mathbf{r})(\sigma_2 \cdot \mathbf{r})}{r^2} - \sigma_1 \cdot \sigma_2. \tag{2}$$

In Fig. 3(a)–3(e), DWBA calculated cross sections for the low-lying quartet states and the 4^- state are compared with the measured values. The contribution from each term of Eq. (1) is shown separately.

For the ranges of the Yukawa function in the τ, $\sigma\tau$, and $T\tau$ terms (i.e., R_τ, $R_{\sigma\tau}$, and $R_{T\tau}$), values of 1.415 fm, 1.415 fm, and 0.878 fm [29] were used, respectively. For the spin-orbit part, the potential range $R_\tau^{\rm LS}$ of 1.2 fm was used following Ref. [28]. The strengths of the effective interactions, V_τ, $V_{\sigma\tau}$, $V_{T\tau}$, and $V_\tau^{\rm LS}$ were treated as free parameters and optimized to reproduce the measured cross sections by the procedure described below.

The potential depths and ranges of the effective interactions determined in the present analysis are summarized in Table II. Due to the unnatural parity characteristics, strong contributions from the $\sigma\tau$ and $T\tau$ terms are expected for the excitation of the 0^- state [28]. Therefore, a good fit of the 0^- cross sections were given priority resulting in the $V_{\sigma\tau}$ and $V_{T\tau}$ strengths of -2.3 MeV and -3.3 MeV/fm^2, respectively. The $V_{\sigma\tau}$ value is smaller than the values of -3.0 MeV previously reported for the $A = 13$ system [30], and -3.9 MeV and -4.2 MeV for the $A = 11$ system [31], but larger than the value of -2.1 MeV for the $A = 208$ system [32]. The present value of $V_{T\tau}$ is larger than those given in these references (-2.5 MeV/fm^2 [31] and -2.0 MeV/fm^2 [32]).

As seen in Fig. 3(a), the DWBA calculation for the 0^- state reproduces the experimental angular distribution well at $\theta_{\rm c.m.} < 10^\circ$ ($q < 1.2$ fm^{-1}), but not so well at larger angles. In this region where the contribution of the $T\tau$ term is larger, the pion effect is expected. Therefore, the validity of this term was carefully examined using the stretched 4^- state, since it is known that the $T\tau$ term dominates the cross sections for high-spin states of unnatural parities [28,33,34]. It should be noted that the strength of the $T\tau$ term has not been well determined at 140 MeV/nucleon, simply because it is not well examined. As shown in Fig. 3(e), the calculated 4^- cross sections well reproduce both the shape of the measured angular distribution

TABLE II. The parameters of the effective interactions. The ranges are from Refs. [28,29]. The depths are from the present analysis. For details, see text.

	τ	$\sigma\tau$	$LS\tau$	$T\tau$
R_α	1.415	1.415	1.2	0.878
V_α	1.0	−2.3	−1.3	−3.3

as well as its maximum value using the $V_{T\tau}$ value determined here. From this comparison we suggest that the obtained $T\tau$ strength is realistic.

As written above, the SM wave functions for the 0^-, 1^-, 2^-, and 3^- states all consist of a main configuration and other residual configurations (see Table I). In order to examine the effect of ambiguity in the wave function of the 0^- state, calculations using all the configurations $[(2s_{1/2}, p_{1/2}^{-1})$ and $(d_{3/2}, p_{3/2}^{-1})]$ and only the main $[(2s_{1/2}, p_{1/2}^{-1})]$ configuration were compared. At the small q region, in which the $\sigma\tau$ term contributes strongly, the calculated cross sections including all configurations were larger than the values using only the main configuration by a factor of 1.3. On the other hand at the third maximum peak seen at $\theta_{\mathrm{c.m.}} \approx 13^\circ$, where the pion effect is expected, the difference was less than 5%. It should be noted that such ambiguity is not expected for the stretched 4^- state, since in principle pure wave function can be assumed. For the 1^-, 2^-, and 3^- states, the peak values using all the configurations differ from those using only main configurations by factors of 1.4, 0.7, and 0.9, respectively.

As mentioned above, in the 0^- angular distribution measured by the (p,n) reaction at 35 MeV [10], a second peak that was not predicted by the DWBA calculation was observed at a momentum transfer q larger than 1.4 fm^{-1}. A possible contribution of the condensed pion field was suggested. In the present (^{3}He,t) measurement at a higher incident energy of 140 MeV/nucleon, where the reaction mechanism becomes simpler, a peak was also observed in the corresponding q region ($\theta_{\mathrm{c.m.}} > 12^\circ$) [see Fig. 3(a)]. Unlike in the (p,n) reaction at 35 MeV, the existence of the peak was reproduced by the DWBA calculation. However, the measured cross sections at the peak region were larger by about a factor of 2–2.5. As mentioned above, cross sections larger by about 20% were also observed in the recent ^{16}O(p,p') measurement at $E_p = 295$ MeV [9]. This was attributed to the presence of a pionic enhancement in nuclei. The larger cross sections in our measurement may also suggest a pionic enhancement. However, as we will discuss below, since the DWBA calculations for other J states could not always reproduce the experimental cross sections well, we should avoid the conclusion that there is a contribution from the condensed pion field.

The other parameters of the effective interactions were obtained as follows. The V_τ strength of 1.0 MeV was determined from the empirical ratio of the GT and Fermi unit cross sections, the R^2 value of 5.2 [35], where neglecting the distortion effect R^2 is defined by $|V_{\sigma\tau}/V_\tau|^2$. The V_τ^{LS} strength of -1.3 MeV was determined by reproducing the measured cross sections for the 2^- state together with the obtained $V_{\sigma\tau}$ and $V_{T\tau}$ values.

The calculation for the 2^- state shows quite good agreement, as shown in Fig. 3(c). The magnitude, but not the shape, of the measured cross section for the 3^- state was reproduced by the calculation as shown in Fig. 3(d). The cross sections for the 1^- state [Fig. 3(b)] was not well reproduced, although the configuration of the 1^- state is expected to be similar to the 0^- g.s.

Up to now, the parameters of the effective $LS\tau$ term in the (^{3}He,t) reaction are not well known. In Ref. [28], a strong spin J dependence of the V_τ^{LS} strengths of more than one order of magnitude was suggested at lower energies. In order to examine the validity of the $LS\tau$ term, DWBA calculations for a Fermi transition using the obtained V_τ^{LS} and V_τ strengths were compared with the measured cross sections. For this purpose, the Fermi transition in the ^{30}Si(^{3}He,t)^{30}P reaction at 140 MeV/nucleon [36] is used. The measurements were performed in the laboratory angular range of 0° to 5°. A self-supporting $^{\mathrm{nat}}$Si target with 2.4 mg/cm^2 areal density was used, which includes 3.1% of ^{30}Si. In Fig. 4, results of the calculations are shown together with the measured values. Only with the τ contribution, the experimental decrease in cross section as a function of the scattering angle was well reproduced. By including the $LS\tau$ term, however, a maximum of the angular distribution appeared at $\theta_{\mathrm{c.m.}} \approx 3^\circ$. This fact may suggest that the $LS\tau$ term with only one range and the fixed V_τ^{LS} value might not be realistic and more sophisticated multirange calculations are needed. However, for simplicity, we performed the optimization within the framework of one-range interaction in the present analysis.

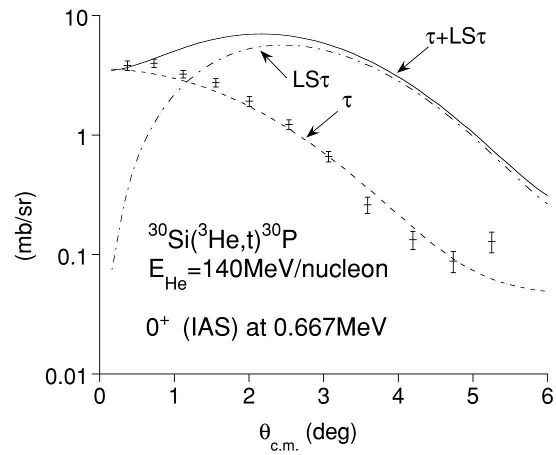

FIG. 4. Result of the DWBA calculation for the Fermi transition from the ^{30}Si g.s. to the IAS in ^{30}P [36] using the phenomenological effective interaction. Without the $LS\tau$ contribution, the measured cross sections were better reproduced.

The poor reproductions of the angular distributions of the 1^- and 3^- states can also be attributed to this $LS\tau$ term, because relatively strong contributions are expected from this term as shown in Fig. 3(b) and (d). It should be noted that even by changing the V_τ^{LS} strength from -5 to +5 MeV, the 1^- and 3^- angular distributions were not reproduced.

By using the peak deconvolution software, the intrinsic peak widths Γ of the low-lying quartet states were extracted. The Γ values from the 0° and 6° spectra are shown in Table III. From the difference of Γ values for the 2^- states at 0° and 6°, we estimate that the uncertainties in these values are 16 keV. Within this error, consistent results were obtained from the spectra taken at both angles. The obtained widths for the 0^- and 1^- states also agree with the results given in Ref. [12] as shown in Table III. For the 3^- state in the 0° spectrum and the 0^- and 1^- states in the 6° spectra, the Γ values could not be determined reliably because of the poor statistics and relatively weak strengths [see Fig. 2(a) and 2(b)].

TABLE III. The measured peak widths Γ for the low-lying states in ^{16}F nuclei. Corresponding values reported in Ref. [12] are also shown.

E_x (keV)	J^π	Γ (keV)		
		at 0°	at 6°	Ref. [12]
g.s.	0^-	18(16)		≈25
193	1^-	87(16)		≈95
424	2^-	16(16)	≈0(16)	
721	3^-		12(16)	

IV. SUMMARY

A ^{16}O(^{3}He,t) experiment was performed at an incident beam energy of 140 MeV/nucleon using the high energy resolution Grand Raiden spectrometer. By applying the dispersion matching technique using the WS beamline and the Grand Raiden spectrometer, an energy resolution of 65 keV was achieved. The scattering angles were measured precisely by applying the angular dispersion matching and the over-focus mode procedures. Owing to the high energy resolution, the low-lying states were clearly resolved for the first time at intermediate energies. Angular distributions of cross sections for the discrete spin-dipole states, the 0^- ground state, the 1^- state at 0.193 MeV, and the 2^- state at 0.424 MeV, were measured together with the 3^- state at 0.721 MeV and the stretched 4^- state at 6.372 MeV in the angular range of $\theta_{\rm lab} = 0°$ to 14°. In addition, the decay widths were obtained for the 0^-, 1^-, 2^-, and 3^- states. The optical model potential parameters of ^{3}He on ^{16}O were determined by fitting the measured cross sections for elastic scattering.

The measured cross sections were compared with the results of DWBA calculations. As a result of the shell-model calculations, very pure configurations of the wave functions for all negative parity states were obtained. The parameters of the effective interactions $V_{\sigma\tau}$, $V_{T\tau}$, and $V_\tau^{\rm LS}$ were determined in order to reproduce the measured angular distributions of the 0^- and 2^- states. The obtained value of $V_{\sigma\tau} = -2.3$ MeV lies between the values suggested in the previously published papers, while $V_{T\tau} = -3.3$ MeV is larger than the previous results. The 4^- angular distribution was used to validate the $T\tau$ term because a strong tensor contribution is expected for that distribution. The newly determined $V_\tau^{\rm LS}$ value, however, seems to be ambiguous.

In the larger momentum transfer region of the 0^- state, the experimental cross sections were larger by a factor of about 2–2.5 compared with the calculated ones. This difference may suggest the contribution from the pionic enhancement. In order to extract a decisive conclusion, however, more elaborated DWBA calculations are needed.

ACKNOWLEDGMENTS

The ^{16}O(^{3}He,t) experiment was performed at RCNP. We are grateful to the RCNP accelerator group, especially to Prof. T. Saito for their effort in providing a high-quality ^{3}He beam indispensable for the realization of the matching conditions. We highly appreciate the valuable suggestions of Prof. B.A. Brown regarding the shell-model calculations using the code OXBASH.

[1] W. G. Love and M. A. Franey, Phys. Rev. C **24**, 1073 (1981); M. A. Franey and W. G. Love, *ibid*. **31**, 488 (1985).
[2] W. M. Alberico, M. Ericson, and A. Molinari, Nucl. Phys. **A379**, 429 (1982).
[3] F. Osterfeld, Rev. Mod. Phys. **64**, 491 (1992).
[4] J. W. Watson, B. D. Anderson, A. R. Baldwin, C. C. Foster, D. Lamm, R. Madey, Marco R. Plumley, and P. J. Pella, Nucl. Phys. **A577**, 79c (1994).
[5] T. Kawabata, T. Ishikawa, M. Itoh, M. Nakamura, H. Sakaguchi, H. Takeda, T. Taki, M. Uchida, Y. Yasuda, M. Yosoi, H. Akimune, K. Yamasaki, G. P. A. Berg, H. Fujimura, K. Hara, K. Hatanaka, J. Kamiya, T. Noro, E. Obayashi, T. Wakasa, H. P. Yoshida, B. A. Brown, H. Fujita, Y. Fujita, Y. Shimbara, H. Ueno, M. Fujiwara, K. Hosono, A. Tamii, and H. Toyokawa, Phys. Rev. C **65**, 064316 (2002).
[6] K. Hosono, M. Fujiwara, K. Hatanaka, H. Ikegami, M. Kondo, N. Matsuoka, T. Saito, S. Matsuki, K. Ogino, and S. Kato, Phys. Rev. C **30**, 746 (1984).
[7] R. Sawafta, A. D. Bacher, G. P. A. Berg, J. Lisantti, C. Olmer, B. K. Park, E. J. Stephenson, S. W. Wissink, D. Frekers, J. D. King, M. Munro, and J. Piekarewicz, IUCF Scientific and Technical Report, May 1988–April 1989, p. 19.
[8] J. D. King, D. Frekers, R. Abegg, R. E. Azuma, L. Buchmann, C. Chan, T. E. Drake, R. Helmer, K. P. Jackson, L. Lee, C. A. Miller, E. Rost, R. Sawafta, R. Schubank, S. S. M. Wong, S. Yen, and X. Q. Zhu, Phys. Rev. C **44**, 1077 (1991).
[9] T. Wakasa, G. P. A. Berg, H. Fujimura, K. Fujita, K. Hatanaka, M. Ichimura, M. Itoh, J. Kamiya, T. Kawabata, Y. Kitamura, E. Obayashi, H. Sakaguchi, N. Sakamoto, Y. Sakemi, Y. Shimizu, H. Takeda, M. Uchida, Y. Yasuda, H. P. Yoshida, and M. Yosoi, Phys. Lett. **B632**, 485 (2006).
[10] H. Orihara, S. Nishihara, K. Furukawa, T. Nakagawa, K. Maeda, K. Miura, and H. Ohnuma, Phys. Rev. Lett. **49**, 1318 (1982).
[11] R. Madey, B. S. Flanders, B. D. Anderson, A. R. Baldwin, W. Bertozzi, T. Chittrakarn, J. R. Comfort, J. M. Finn, C. C. Foster, C. Hyde-Wright, J. J. Kelly, C. Lebo, H. Orihara, W. Pairsuwan, and J. W. Watson, Phys. Rev. C **56**, 3210 (1997).
[12] W. A. Sterrenburg, S. Brandenburg, J. H. van Dijk, A. G. Drentje, M. B. Greenfield, M. N. Harakeh, H. Riezebos, H. Sakai, W. Segeth, S. Y. van der Werf, and A. van der Woude, Nucl. Phys. **A420**, 257 (1984).
[13] M. Fujiwara, H. Akimune, I. Daito, H. Fujimura, Y. Fujita, K. Hatanaka, H. Ikegami, I. Katayama, K. Nagayama, N. Matsuoka, S. Morinobu, T. Noro, M. Yoshimura, H. Sakaguchi, Y. Sakemi, A. Tamii, and M. Yosoi, Nucl. Instrum. Methods Phys. Res. A **422**, 484 (1999).

[14] Y. Fujita, Y. Shimbara, A. F. Lisetskiy, T. Adachi, G. P. A. Berg, P. von Brentano, H. Fujimura, H. Fujita, K. Hatanaka, J. Kamiya, T. Kawabata, H. Nakada, K. Nakanishi, Y. Shimizu, M. Uchida, and M. Yosoi, Phys. Rev. C **67**, 064312 (2003).
[15] I. Miura *et al.*, RCNP Annual Report 1991, Osaka University, p. 149.
[16] T. Wakasa, K. Hatanaka, Y. Fujita, G. P. A. Berg, H. Fujimura, H. Fujita, M. Itoh, J. Kamiya, T. Kawabata, K. Nagayama, T. Noro, H. Sakaguchi, Y. Shimbara, H. Takeda, K. Tamura, H. Ueno, M. Uchida, M. Uraki, and M. Yosoi, Nucl. Instrum. Methods A **482**, 79 (2002).
[17] Y. Fujita, K. Hatanaka, G. P. A. Berg, K. Hosono, N. Matsuoka, S. Morinobu, T. Noro, M. Sato, K. Tamura, and H. Ueno, Nucl. Instrum. Methods Phys. Res. B **126**, 274 (1997).
[18] H. Fujita, Y. Fujita, G. P. A. Berg, A. D. Bacher, C. C. Foster, K. Hara, K. Hatanaka, T. Kawabata, T. Noro, H. Sakaguchi, Y. Shimbara, T. Shinada, E. J. Stephenson, H. Ueno, and M. Yosoi, Nucl. Instrum. Methods A **484**, 17 (2002).
[19] T. Noro *et al.*, RCNP Annual Report 1991, Osaka University, p. 177.
[20] H. Fujita, G. P. A. Berg, Y. Fujita, K. Hatanaka, T. Noro, E. J. Stephenson, C. C. Foster, H. Sakaguchi, M. Itoh, T. Taki, K. Tamura, and H. Ueno, Nucl. Instrum. Methods A **469**, 55 (2001).
[21] H. Fujita (private communication).
[22] R. Schaeffer and J. Raynal (1970), extended version DW81 by J. R. Comfort (1981), updated version (1986).
[23] B. A. Brown, A. Etchegoyen, N. S. Godwin, W. D. M. Rae, W. A. Richter, W. E. Ormand, E. K. Warburton, J. S. Winfield, L. Zhao, and C. H. Zimmerman, NSCL Report No. 524; B. A. Brown (private communication).
[24] E. K. Warburton and B. A. Brown, Phys. Rev. C **46**, 923 (1992).
[25] J. Raynal, computer code ECIS-88 NEA-0850/08.
[26] J. Kamiya, K. Hatanaka, T. Adachi, K. Fujita, K. Hara, T. Kawabata, T. Noro, H. Sakaguchi, N. Sakamoto, Y. Sakemi, Y. Shimbara, Y. Shimizu, S. Terashima, M. Uchida, T. Wakasa, Y. Yasuda, H. P. Yoshida, and M. Yosoi, Phys. Rev. C **67**, 064612 (2003).
[27] T. Yamagata, H. Utsunomiya, M. Tanaka, S. Nakayama, N. Koori, A. Tamii, Y. Fujita, K. Katori, M. Inoue, M. Fujiwara, and H. Ogata, Nucl. Phys. **A589**, 425 (1995).
[28] S. van der Werf, S. Brandenburg, P. Grasdijk, W. A. Sterrenburg, M. N. Harakeh, M. B. Greenfield, B. A. Brown, and M. Fujiwara, Nucl. Phys. **A496**, 305 (1989).
[29] R. Schaeffer, Nucl. Phys. **A164**, 145 (1971).
[30] H. Fujimura, H. Akimune, I. Daito, M. Fujiwara, K. Hara, K. Y. Hara, M. N. Harakeh, F. Ihara, T. Inomata, K. Ishibashi, T. Ishikawa, T. Kawabata, A. Tamii, M. Tanaka, H. Toyokawa, T. Yamanaka, and M. Yosoi, Phys. Rev. C **69**, 064327 (2004).
[31] T. Kawabata, H. Akimune, H. Fujimura, H. Fujita, Y. Fujita, M. Fujiwara, K. Hara, K. Y. Hara, K. Hatanaka, T. Ishikawa, M. Itoh, J. Kamiya, S. Kishi, M. Nakamura, K. Nakanishi, T. Noro, H. Sakaguchi, Y. Shimbara, H. Takeda, A. Tamii, S. Terashima, H. Toyokawa, M. Uchida, H. Ueno, T. Wakasa, Y. Yasuda, H. P. Yoshida, and M. Yosoi, Phys. Rev. C **70**, 034318 (2004).
[32] R. G. T. Zegers, H. Abend, H. Akimune, A. M. van den Berg, H. Fujimura, H. Fujita, Y. Fujita, M. Fujiwara, G. Galés, K. Hara, M. N. Harakeh, T. Ishikawa, T. Kawabata, K. Kawase, T. Mibe, K. Nakanishi, S. Nakayama, H. Toyokawa, M. Uchida, T. Yamagata, K. Yamasaki, and M. Yosoi, Phys. Rev. Lett. **90**, 202501 (2003).
[33] A. Fazely, B. D. Anderson, M. Ahmad, A. R. Baldwin, A. M. Kalenda, R. J. McCarthy, J. W. Watson, R. Madey, W. Bertozzi, T. N. Buti, J. M. Finn, M. A. Kovash, B. Pugh, and C. C. Foster, Phys. Rev. C **25**, 1760 (1982).
[34] K. Hosono, N. Matsuoka, K. Hatanaka, T. Saito, T. Noro, M. Kondo, S. Kato, K. Okada, K. Ogino, and Y. Kadota, Phys. Rev. C **26**, 1440 (1982), and references therein.
[35] Y. Fujita, J. Phys.: Conf. Ser. **16**, 107 (2005).
[36] H. Fujita *et al.*, OULNS Annual Report 2007, Osaka University (unpublished).